Physical Modelling in Geotechnics – 6th ICPMG '06 – Ng, Zhang & Wang (eds)
© 2006 Taylor & Francis Group, London, ISBN 0-415-41586-1

The use of centrifuge tests in the study of arching

H.Y. Chua
Cambridge University Engineering Department, UK

M.D. Bolton
Schofield Centre, Cambridge University Engineering Department, UK

ABSTRACT: The horizontal arching mechanism transfers horizontal earth pressures acting on flexible retaining wall panels to stiffer neighbouring elements via soil shear stresses. In this research, the horizontal arching mechanism and lateral displacements of fixed cantilever walls in a model basement are investigated using centrifuge tests. A series of six tests was carried out at 45 gravities where the panel widths and thicknesses around the model basement were varied, so that the effects of panel geometry and stiffness on horizontal arching could be studied. It is shown that panel crest displacements and base bending moments of the most flexible, narrow panels can be an order of magnitude smaller than conventional active earth pressure calculations would allow. It is suggested that the reduction of earth pressure acting on a panel is directly correlated to the mobilized soil shear strength and hence, soil shear strain. Earth pressure coefficients K are plotted against panel displacements normalized by the panel width, u/B, to simulate the reduction of K with increasing soil strain. An idealized K-u/B curve is introduced, characterised by a reference distortion $(u/B)_{ref}$ beyond which fully plastic soil arching can be inferred, and which is related to the corresponding reference shear strain γ_{ref} at which soil strength is fully mobilized in element tests.

1 INTRODUCTION

It is widely acknowledged that the earth pressure distribution on retaining walls is a three-dimensional soil-structure interaction problem. Previous research has established the influence of wall installation effects, wall stiffness and support conditions, and wall friction, on earth pressure distributions. The horizontal and vertical arching mechanisms and their effect on pressure distributions on retaining walls, have since been identified to be of similar importance. While this has been the subject of much discussion, it has not yet led to practical guidance for designers.

The focus of this paper will be on the design benefits that may be reaped from the horizontal arching mechanism, a phenomenon where wall elements in plan view will carry disproportionate amounts of earth thrust depending on their relative deflection. Current earth pressure theories are based on walls of infinite width, deforming in plane strain. The neglect of arching may lead to unnecessary concern about the failure of flexible retaining systems that are supported by stiff but intermittent supports.

A study was made of the distribution of horizontal earth pressures on a cantilever retaining wall system, investigating the effect of panel geometry. Previous researchers (Fang & Ishibashi 1986, Potts & Fourie 1986, Bolton & Powrie 1987) have usually focussed on the plane strain problem. Here, six parametric tests were carried out with a retaining wall system simulating a 11.25 m deep basement excavation at prototype scale, with various panel widths and bending stiffnesses (see Figure 1 and Table 1). The model basement was constructed from aluminium alloy, but Table 2 indicates the equivalent thickness of the panels had they been constructed of reinforced concrete.

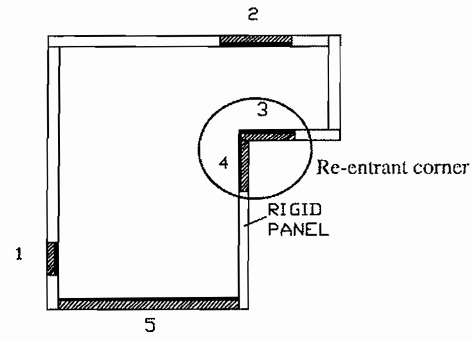

Figure 1. Plan view of model basement (retaining system).

Table 1. Widths and thickness of panels used in model basement (model scale).

		Thickness (mm)		
Panel no.	Width (mm)	Flexible HYC2, HYC5	Med stiff HYC3, HYC6	Stiff HYC4, HYC7
1	40	4.76	6.35	9.53
2	80	4.76	6.35	9.53
3	60	4.76	6.35	9.53
4	60	4.76	6.35	9.53
5	200	4.76	6.35	9.53

Table 2. Thickness of concrete panels of equivalent stiffness at prototype scale.

Thickness of aluminium alloy panels at model scale (mm)	Thickness of concrete panels at prototype scale (mm)
4.76	302
6.35	403
9.53	604
12.7	806

Excavation was simulated by the incremental removal of a heavy fluid from inside the model basement. The horizontal displacements of the wall crests, and bending moments near their fixed bases, were measured as excavation was carried out. In addition, horizontal earth pressures near the tops and bottoms of the panels were measured using miniature earth pressure cells.

The model retaining system, the excavation procedure and results obtained from the centrifuge tests have been described in Chua & Bolton (2005). It was shown that horizontal earth pressures were reduced to a fraction of the active earth pressures as the retaining walls deflected under excavation. The next section will summarize the method by which that data of panel displacements, bending moments, and horizontal earth pressures were converted, separately, into equivalent earth pressure coefficients. It should be noted that results recorded on panels at the re-entrant corner, shown in Figure 1, will not be addressed in this paper.

2 DERIVATION OF K-VALUES

Data gathered can best be understood in relation to current earth pressure theories if an equivalent triangular earth pressure diagram is assumed, whose gradient is associated with an equivalent earth pressure coefficient. A chart can then be made of predicted wall deflections, each calculated by assuming some constant earth pressure coefficient on the active side of

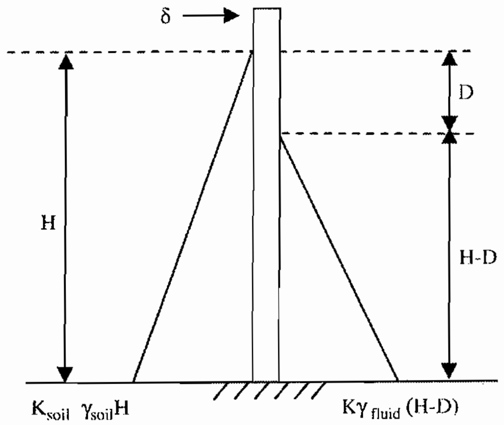

Figure 2. Theoretical loading model of cantilever used in calculations.

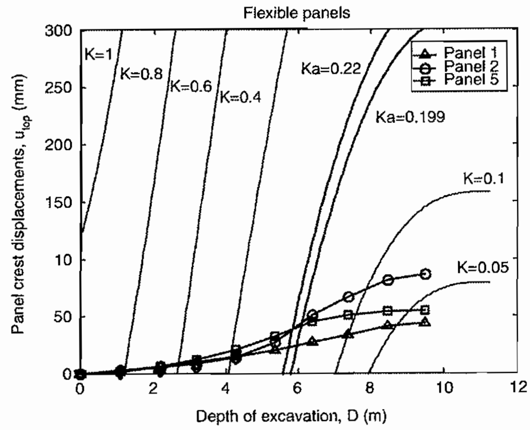

Figure 3. Superimposition of recorded flexible panel displacements on predicted panel displacements (results from test HYC5).

the wall panel and, similarly, a hydrostatic fluid pressure distribution beneath the simulated excavation on the resisting side. The recorded panel crest displacements during the process of excavation can then be superimposed onto the same chart, so that a progression of equivalent earth pressure coefficients can be inferred.

Figure 2 shows the theoretical model of a fixed cantilever that was used in calculations. Varying earth pressure coefficient (K) values were used to derive different deflection values, whilst K_{fluid} is always unity. Figure 3 then shows the outcome for flexible panel displacements. All three panels (narrow, medium and wide) display paths that track quickly across K values from 1 down to the theoretical active values of 0.22 for a perfectly smooth wall and 0.20 for a wall with

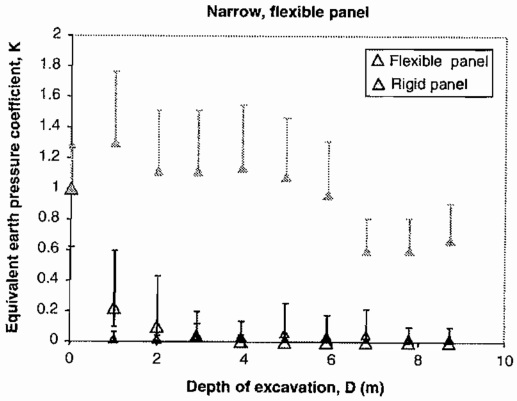

Figure 4. Equivalent earth pressure coefficients, K, from pressure cell data at 2.25 m from the ground surface on panel 1 (flexible panel).

roughness $\delta = 20°$. The soil internal angle of friction was estimated from its relative density using Bolton's (1986) equation for triaxial strain. Thus K-values may be deduced from panel displacements (and given the notation K_u).

Similarly, it was found that the K-values inferred from panel bending moments (K_M) dropped very rapidly as excavation was carried out, and for flexible panels the ultimate K_M-value was only 5% of active earth pressures – see Chua & Bolton (2005) for details. This is further supported by pressure cell data, where measured horizontal pressures σ_h at the panel tops were found to be very small. Figure 4 presents the measured pressure σ_h normalized by the initial horizontal pressure σ_{hi}, to obtain another equivalent K-factor.

An interesting feature observed from the pressure data was that recorded earth pressures at the base of the panels were also very small. This contradicts previous suggestions that earth pressures at a rotating panel base remain "locked" at magnitudes approximately equal to $K_0\gamma H$, and instead agrees with Paik & Salgado's (2003) proposal that vertical arching reduces horizontal pressures to small fractions of their original values at the panel base.

In general however, experimental results showed that the narrowest panels attracted the least pressure compared to wider panels. Meanwhile, larger earth pressures were recorded on stiffer panels as compared to more flexible ones. These corresponding results are not shown here but may be referred to in Chua & Bolton (2005).

3 THE MOBILIZATION OF HORIZONTAL ARCHING

The experimental results have indicated that reducing panel width B and panel stiffness EI both enhance

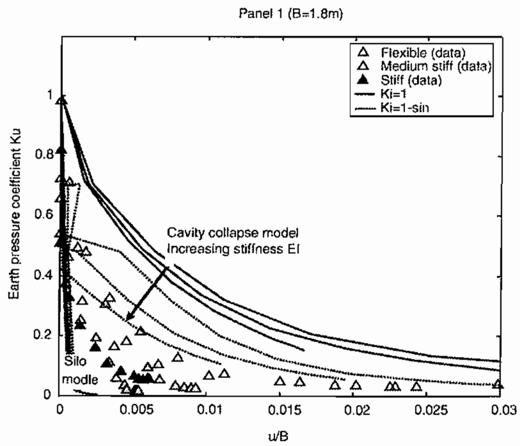

Figure 5. Comparison of predicted values and experimental data for panel displacements using both cavity collapse and silo models; Ki refers to the initial earth pressure coefficient.

horizontal arching. However, conclusions derived from data alone may be insubstantial and thus need to be validated and normalized through the application of the principles of soil mechanics.

Although a theory for horizontal arching is outside the scope of this paper, it has been shown that soil models incorporating the kinematics and equilibrium of cylindrical cavity collapse, or of the displacements and pressures in a silo, may be used to assist in the explanation of soil arching mechanisms. Both theories are detailed in Chua (2005), where it was suggested that the ability of the soil to arch was dependent on the mobilization of the soil shear strength, and thus of the soil shear strain. The analyses were carried out by dividing the soil behind the panels into infinitesimal horizontal laminae, and assuming that the soil was perfectly homogeneous and in an initially isotropic state. As the panels deflected with excavation, it was deduced that the mobilized soil shear strain at any point will be a linear function of the ratio of the panel displacement u divided by the panel width B. The higher the mobilized strain, the higher must be the magnitude of pressure reduction. It was then found that plotting the derived earth pressure coefficients K_u and K_M against the parameter u/B was useful as a representation of the reduction in pressure with mobilized soil strain.

Figure 5 shows predicted K_u values plotted against input u/B values. These theoretical results were generated through pressure-displacement curves obtained from the soil theories, which were then incorporated into a numerical solution for elastic cantilever deflection. The numerical analyses then enabled the calculation of panel displacements, bending moments and horizontal earth pressures. The K_u values seen in Figure 5 were inferred using the same method used for the experimental data. It can be seen that plotting K against u/B consolidates the data into a relatively narrow band, for both the theoretical results and experimental data.

The two theories provided upper and lower-bound solutions to the experimental data. The cavity collapse model, in particular, showed promise in its ability to reflect the reduction in the pressure acting on the flexible panel as it displaces relative to its rigid neighbors. The cavity collapse solution presumably offers an empirical lower-bound because there is an absence of the vertical shear (wall friction) transfer mechanism that would have contributed to further pressure reductions.

4 NORMALIZATION OF DATA

It has been shown that the dimensionless group u/B provides an adequate consolidation of data onto a single curve. On the other hand, plotting the data against the normalized depth of excavation D/H usefully emphasizes the difference in mobilized K-values caused by differences in panel stiffness.

Figure 6a shows the outcome of plotting data for the narrow panel. This plot incorporates the parameters K (from K_u and K_M) and u/B – parameters that may be useful for the engineer in determining the wall stiffness necessary to limit wall displacement to a specified value. Figure 6b then shows an example of a K–D/H plot for the same panel, where the difference in pressure reduction caused by a difference in panel stiffness is portrayed.

Best-fit lines using the least mean squares method were fitted onto the consolidated experimental data obtained from panel displacements and panel bending moments. The mathematical equations for the best-fit lines are based on a generic Heaviside function, which was chosen due to its versatility in adapting to different curve steepness and shapes. An example equation is shown in Figure 6a.

In plotting the best-fit lines through the data in the form of Figure 6a, it was found that idealized curves may be generated in the style of Figure 7. The shape of the idealized curve is like that of an inverted stress-strain curve. Starting at $K = K_0$, the K-value reduces rapidly until it approaches a value K_{min} at a u/B value $(u/B)_{ref}$. This is taken to relate to a triaxial stress-strain curve in which a reference shear strain γ_{ref} might be defined as the shear strain at which the full soil shear strength ϕ_{max} is mobilized. The same property γ_{ref} should therefore be useful in defining the transition between progressive strength mobilization and fully plastic behavior in the boundary value problem, where $(u/B)_{ref} \propto \gamma_{ref}$.

For a medium dense sand ($R_D = 55$ to 65%, as used in these experiments) and an initial isotropic stress state of 170 kPa, Asaka *et al.* (2003) show that

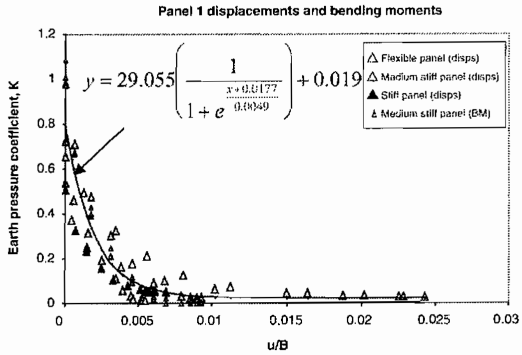

Figure 6a. Best-fit curve of K versus u/B for experimental data from panel 1 (narrow panel).

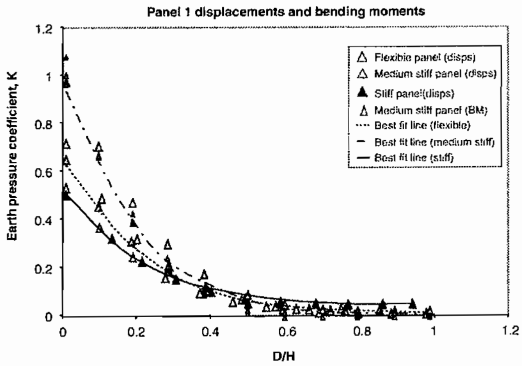

Figure 6b. Best-fit curve of K versus D/H for experimental data from panel 1 (narrow panel).

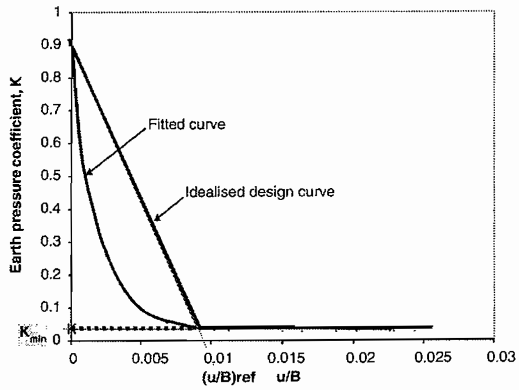

Figure 7. Fitted and idealised K-u/B curve showing $(u/B)_{ref}$ and K_{min}.

$\gamma_{ref} \approx 0.02$. The average of our experimental data gave $(u/B)_{ref} \approx 0.006$. Accordingly,

$$\left(\frac{u}{B}\right)_{ref} \approx 0.3\gamma_{ref} \qquad (1)$$

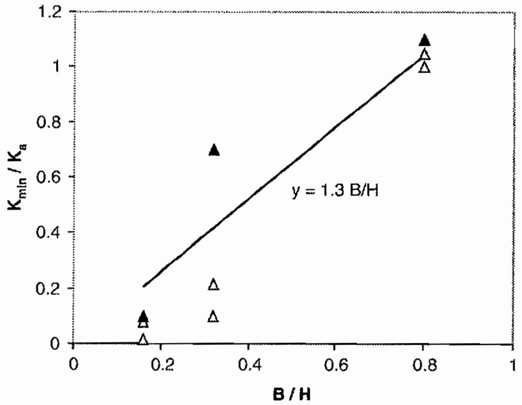

Figure 8. $\alpha = (K_{min}/K_a)$ versus normalized panel width B/H.

It was also found from experimental data that the value of K_{min} is roughly proportional to the panel width. Defining an arching factor $\alpha = K_{min}/K_a$ against the panel width normalized by panel height, B/H, we can plot the data of fully developed arching from the tests as shown in Figure 8. A convenient regression line fitted through the origin gives:

$$\alpha = 1.3\frac{B}{H} \tag{2}$$

It may therefore be concluded that the limiting B/H value is 0.8, beyond which there is negligible horizontal arching, and classical plane strain solutions should apply.

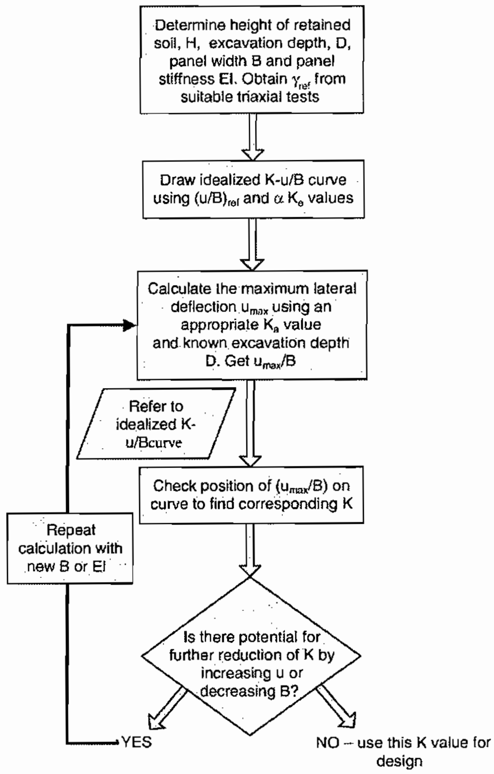

Figure 9. Proposed design sequence for small earth pressures caused by arching.

5 DESIGN PROCEDURE

The proposed sequence of design is intended to help engineers derive the minimum earth pressure expected to act on the flexible elements of a retaining system, depending on the wall displacement, which may be used as a controlling parameter. Where ground settlements and wall lateral movements are not of concern, maximum arching may be harnessed. It should be noted that results shown here are for medium-dense soils; the increase or reduction in soil density may affect the K_{min} and B/H limitations. The design sequence is shown in Figure 9.

Worked example:

Consider a flexible cantilever panel of width $B = 2$ m within a stiff retaining wall system – the panel might be temporary works, or might be flanked by transverse wall segments onto which lateral forces may arch. It is to be designed to retain 5 m of dense sand ($\gamma_{soil} = 15$ kN/m^3, $\phi_{max} = 40°$), with a horizontal ground surface. The maximum allowable panel deflection is 25 mm and the panel stiffness is to be chosen.

1. Choose a reinforced concrete panel of thickness $t = 300$ mm, $E = 25$ GPa. Bending stiffness $EI = 1.13 \times 10^8$ Nm^2.
2. From typical drained triaxial tests, estimate $\gamma_{ref} = 0.01$. Draw idealized bilinear K-u/B curve starting with $K_i = 1$. K drops down to zero at $(u/B)_{ref} = 0.3\gamma_{ref} = 0.003$, with the line equation $K = -333(u/B) + 1$. K is asymptotic at αK_a, where $\alpha = (1.3)(2/5) = 0.52$. $K = 0.52$ when $(u/B) = 0.0014$. Note then that u to mobilize full arching is 2.8 mm, which would be acceptable, since much less than 25 mm.
3. Using Mayniel's chart (say wall friction $\delta = 24°$), find $K_a = 0.20$. Assume there will be sufficient displacement to mobilize $K_{min} = \alpha K_a = 0.104$.
4. Calculate wall displacement u using a triangular earth pressure distribution with $K = 0.104$ and excavation depth $D = 5$ m.
5. For the cantilever panel, $u_{max} = wH^4/30EI$, where $w = K\gamma HB$. Computed $u_{max} = 3$ mm which is sufficient for full arching, and is structurally acceptable.

Soil arching enables engineers to use lower earth pressure coefficients in their design of flexible retaining wall panels, on condition that there are stiff adjacent sections onto which pressures can arch. Previous work by Liang & Zeng (2002) considered the potential of the soil arching mechanism around drilled shafts for slope stabilization. They concluded that soil arching is destroyed when a pile spacing to pile diameter (s/d) ratio of 8 is employed. This suggests that the width of adjacent stiff supports should exceed B/8, but this needs to be validated through further tests.

6 CONCLUSIONS

Six centrifuge tests were conducted in this research project, which enabled a more detailed analysis of the horizontal arching mechanism using experimental data. In these tests, deep excavations around a model basement were simulated, where panel deflections, bending moments and horizontal earth pressures were measured. A simple mechanical model of an elastic cantilever beam was used to infer earth pressure coefficient (K) values from experimental data. It was observed that K-values dropped to far below classical active earth pressure values as excavations progressed.

Based on two different theoretical models, it was then postulated that the magnitude of soil arching was a function of soil shear strain, and thus correlating to the parameter u/B where u is the panel displacement and B is the panel width. A parameter $(u/B)_{ref}$ was proposed as an indicator of the soil achieving its full arching potential. Inferred values from experimental data on medium dense sand indicated that earth pressures dropped to a minimum when $(u/B)_{ref} \approx 0.006$, which might be generalised as $(u/B)_{ref} \approx 0.3\gamma_{ref}$, where γ_{ref} is the shear strain observed to mobilize full strength in an element test. In comparative plane strain walls, where soil shear strain $\gamma \approx 2(u/H)$ following Bolton and Powrie (1987), it would be expected that $(u/H)_{ref} \approx 0.5\gamma_{ref}$ for full mobilisation of active pressures. Since $B < H$, horizontal arching is fully mobilized at smaller wall displacements than with conventional plane wall rotations.

It was further shown that narrow, flexible panels promoted more arching compared to wider, stiffer panels. An arching factor α was proposed, where conventional K_a values may be multiplied by α to produce smaller active earth pressures. It was found that α was a function of B/H where H is the height of the retained soil, and that the average value of α obtained from the centrifuge tests was 1.3B/H.

Based on this observation, the limiting value of B/H, beyond which arching ceases to occur, is 0.8. Using soil arching, engineers are able to take advantage of smaller earth pressures given the same amount of limiting wall deflection, if neighbouring rigid wall sections are available to receive the arched thrust.

Further centrifuge tests may be carried out to derive the optimum support widths needed in relation to flexible panel widths, to obtain complete design guidelines for retaining systems promoting horizontal arching.

REFERENCES

Asaka, Y., Tokimatsu, K., Iwasaki, K. & Shamoto, Y. 2003. Simple stress-strain relation based on stress-path behavior in strain-path controlled triaxial tests. *Soils and Foundations* 43(2): 55–68.

Bolton, M.D. & Powrie, W. 1987. The collapse of diaphragm walls retaining clay. *Géotechnique* 37(3): 335–353.

Chua, H.Y. & Bolton, M.D. 2005. Modelling of horizontal arching on retaining walls. *Proceedings of the 16th International Conference of Soil Mechanics and Geotechnical Engineering, Osaka* 3: 1455–1458.

Chua, H.Y. 2005. *Horizontal arching on retaining structures.* PhD thesis, University of Cambridge.

Fang, Y-S. & Ishibashi, I. 1986. Static earth pressure with various wall movements. *Journal of Geotechnical Engineering ASCE* 112(3): 317–333.

Liang, R. & Zeng, S. 2002. Numerical study of the soil arching mechanism in drilled shafts for slope stabilization. *Soils and Foundations* 42(2): 83–92.

Paik, K.H. & Salgado, R. 2003. Estimation of active earth pressure against rigid retaining walls considering arching effects. *Géotechnique* 53(7): 643–653.

Potts, D.M. & Fourie, A.B. 1986. A numerical study of the effects of wall deformation on earth pressures. *International Journal for Numerical and Analytical Methods in Geomechanics* 10: 383–405.